$f(Q)$ **Gravity and its Cosmological Implications**

By

Ayesha Mahmood

CIIT/FA20-RMT-005/LHR

MS

in

Mathematics

COMSATS University Islamabad

Lahore Campus

Spring, 2022

COMSATS University Islamabad

$f(Q)$ Gravity and its Cosmological Implications

A Thesis Presented to

COMSATS University Islamabad

in partial fulfillment

of the requirement for the degree of

MS (Mathematics)

By

Ayesha Mahmood

CIIT/FA20-RMT-005/LHR

Spring, 2022

$f(Q)$ Gravity and its Cosmological Implications

A Post Graduate Thesis is submitted to the Department of Mathematics as partial fulfillment of the requirement for the award of Degree of MS Mathematics.

Name	Registration Number
Ayesha Mahmood	CIIT/FA20-RMT-005/LHR

Supervisor

Dr. Rabia Saleem
Assistant Professor
Department of Mathematics,
COMSATS University Islamabad (CUI)
Lahore Campus
July, 2022

Final Approval

This thesis titled

$f(Q)$ Gravity and its Cosmological Implications

By

Ayesha Mahmood

CIIT/FA20-RMT-005/LHR

Has been approved

For the COMSATS University Islamabad, Lahore Campus

External Examiner : ______________________

Supervisor : ______________________

(Dr. Rabia Saleem)

HoD/Incharge : ______________________

(Dr. Kashif Ali)

(Mathematics Department, CUI, Lahore Campus)

Declaration

I, **Ayesha Mahmood** with registration number **CIIT/FA20-RMT-005/LHR** hereby declare that I have produced the work presented in this thesis, during the scheduled period of study. I also declare that I have not taken any material from any source except referred to wherever due, that amount of plagiarism is within acceptable range. If a violation of HEC rules on research has occurred in this thesis, I shall be liable to punishable action under the plagiarism rules of the HEC.

Dated : ____________________ ______________________________

(Ayesha Mahmood)

(CIIT/FA20-RMT-005/LHR)

Certificate

It is certified that Ayesha Mahmood with CIIT/FA20-RMT-005/LHR has carried out all the work related to this thesis under my supervision at the Department of Mathematics, COMSATS University Islamabad, Lahore campus and the work fulfills the requirement for award of MS degree.

Dated :____________________

Supervisor:____________________

(Dr. Rabia Saleem)

Assistant Professor

____

(Dr. Kashif Ali)

Head of Department

Department of Mathematics

DEDICATED TO

My Loving Parents, Brothers

and Sisters

ACKNOWLEDGMENTS

All praises to **Allah Almighty**, Who is the Lord and Creator of the universe. Allah gave me knowledge, courage, intelligence and patient to complete my thesis in time. All gratitude is for **Hazrat Muhammad (PBUH)**, who is the greatest inspiration for knowledge and guidance of humanity. I would like to express my deep and sincere gratitude to my competent supervisor **Dr. Rabia Saleem** whose encouragement, motivation and constant guidance helped me to complete this thesis in a systematic manner. I am grateful to my senior **Miss Iqra Shahid** for her valuable guidance, precious time and moral support throughout the research work. I owe thanks to my friends, especially **Miss Naeema Khan** for moral support throughout this period. I can not express my heartiest feelings for my **parents** in words. I thank them for their love, prayers, encouragement and sacrifice. I would like to acknowledge my caring brother **Mr. Ahmad Mahmood** and sister **Miss. Sara Mahmood** for their love and support. I wish to dedicate last lines of this page to my loving father who inspired me throughout of my life; this thesis would have been simply impossible without him. He is everything for me. I would also like to acknowledge **Mr. Mohsin Shad** for his valuable support, time and encouragement throughout my work.

Lahore ***Ayesha Mahmood***

July, 2022 ***CIIT/FA20-RMT-005/LHR***

ABSTRACT

This thesis is devoted to study some cosmic aspects within $f(Q)$ gravity in the context of two different models, the power-law model $f(Q) = Q + \alpha Q^2$, and the exponential model $f(Q) = Qe^{\frac{\lambda Q_0}{Q}}$. To complete the target, a homogenous and isotropic space-time under perfect fluid distribution is considered to develop the dynamical system of equations. We examine the behavior of each model by using some cosmological parameters including, deceleration parameter, square speed of sound, statefinder and $Om(z)$-diagnostic which give results that are compatible with the expanding phenomena of universe. The graphical analysis of square speed of sound justifies the unstability of first model while second model is stable. Using fixed point method, we construct the relevant autonomous system of equations to examine the stability of model for phantom, vacuum, and non-phantom phases. Moreover the study of growth index of matter perturbation in this theory describes that the anisotropic stress is equal to unity, which is the same result obtained in general relativity.

Contents

List of Figures

List of Tables

Chapter 1

Introduction

Theory of special relativity was proposed and published by Albert Einstein in 1905, which is applicable to all physical events happening in inertial frame of reference in the absence of gravity. Later in 1915, he extended it to general relativity (GR) that explains the law of gravitation and its relation with other forces of nature. It explains events in both inertial and non-inertial frames of reference. General relativity is one of the most significant achievements in modern physics. It applies to cosmological and astrophysical phenomenon including astronomy.

Einstein applied his new theory of gravity to the universe as a whole and results led him to consider a finite and static universe. To get compatible results, he injected cosmological constant Λ, in field equations. In 1920, Edwin Hubble made a revolutionary discovery of expanding universe [1]. The light coming from distant galaxies verified that they were all moving away from each other. After that, Einstein set Λ to zero declaring it "no longer necessary and theoretically unsatisfactory". He admitted it "biggest blunder" of his life. The idea of static universe was no longer accepted and a new idea of accelerating cosmos was given by Friedmann.

A branch of Astronomy that deals with the origin, evolution, large scale structure and ultimate fate of cosmos from big-bang to this day and endlessly into the future is known as cosmology. The word cosmology is formed by the union of two Greek words "cosmos" and "logy". The word "cosmos" stands for "Universe" and "logy" means "the study of". In astronomy, we study only the specific celestial objects while cosmology covers the whole cosmos. Cosmologists look into many un-revealed components of the cosmos and assume that a huge part of this cosmos consists of galaxies, planets, clusters and stars. Cosmology also promotes to describe basics of many fascinating phenomena like big-bang, gravitational collapse and end state of standard evolution. It is believed that in today's cosmology, one major discovery is the acceleration in cosmic expansion.

In 1998, two distinct projects, high-z supernova and the supernova cosmology project discovered the accelerating expansion of the cosmos [2, 3]. Both used distant type la supernova to evaluate the acceleration. The uncertain consequence was that the objects in the cosmos are drifting apart from each other at an accelerating rate. If one runs the clock backward, he will quickly realize that in past, galaxies were closer. By moving it back further to the end, one will observe that there were no galaxies anymore. If one keeps on going in past, considering the cosmic scale as big as it is today, it will reduce to an infinite small, hot and dense point dubbed as singularity. That is what, GR, a mathematical tool for understanding the cosmic evolution over millennial timescale, tells us: 13.8 billion years ago, universe as one understands today, was nothing but a singularity, a crucial point which had infinite density. To find an appropriate model for the present cosmos, some preferable reasons for cosmic acceleration have been studied on the large scale. The dark energy (DE) is the main factor which describes this apart from cosmological constant, DE models and modified theories of gravity.

It is discovered that the cosmos enlarges its scale with repulsive force which is not slowing down under normal matter. This strange force with negative pressure (or exotic matter) is called DE which is different from ordinary matter species like radiation and baryons [4, 5]. In physical cosmology and astronomy, there is a mysterious energy called DE that tends to fill all of space and accelerate the expansion of the cosmos. Dark energy can also be explained by the fact that it is a new type of dynamical energy fluid, whose impact on the expansion of the universe is opposite to that of normal matter. So by observations, it is confirmed that our universe is made up of some invisible components, DE, DM and of visible matter. Approximately, our universe constitutes 26.8% of DM and 4.9% of visible matter. Recent supernova type la (SNIa) observation found that DE includes 68.3% of current energy budget of the universe [6].

Dark matter is responsible for structure formation of the universe. When we determine that why cosmos is established the way it is? it swiftly became clear that universe not contain abundant matter only but it is made up of some exotic particles that do not interact with light and matter in a way we expect. Matter exists in two forms: baryonic and non-baryonic. The electromagnetic radiations emitted by stars, cause the photons to spread in every direction through which astronomers can indicate DM. Since light of any wavelength can not be dispersed or absorbed by this matter therefore it is impossible to identify it directly. It is the form of matter that is assumed to prevail because scientists have perceived its gravitational consequences on galaxies and clusters. Dark matter can explain the phenomena of galactic rotation curves and gravitational lensing.

Our cosmos went through three different dominated eras during expansion: radiation, matter, and the DE eras, which can be distinguished by an equation of state (EoS) parameter $\omega = \frac{p}{\rho}$, where p and ρ be the total pressure and energy density of the fluid, respectively. The parametric values, $\omega = \frac{1}{3}, 0$ denote radiation and matter dominated phases, respectively. While $\omega \leq -\frac{1}{3}$ is the minimum requirement for DE paradigm. In addition to DE phases, there are non-phantom $(-1 < \omega < -\frac{1}{3})$, vacuum $(\omega = -1)$ and phantom $(\omega < -1)$ phases.

Some other cosmological parameters are very efficient to describe cosmic expansion and to understand physical behavior of DE and DM. We know that our universe is expanding but rate of expansion is still undetermined. The Hubble parameter (H) is very important to describe the expansion rate of cosmos. While deceleration parameter q, can categorize the accelerating, decelerating and static phases of cosmos. The H and q parameters are good enough to explain the behavior of cosmos in detail but unfit to differentiate between different DE models. In order to resolve this issue, Sahni et al. [7] introduced a pair of new parameters known as statefinder (j, s) and $Om(z)$. Statefinder pair is very helpful in explaining nature of many DE models and in describing how far a model is from ΛCDM model. However, the $Om(z)$ parameter is another diagnostic tool which can distinguish dynamical DE models from ΛCDM (cold dark matter) model with positive and negative slope. Baryons plus CDM is responsible to derive new accelerating cosmology in the framework of GR.

Dark energy and DM are unable to address all of the problems related to accelerating expansion of cosmos. From this point, the explanation of observed acceleration is to be set up in characterization of modified theory of gravity, that must be capable to reproduce the results of GR at scales ranging from microns to astrophysical scales. Generally, the concept of modified theories of gravity came from the modification of Einstein-Hilbert action, where extra terms are involved. Hence, there is enough motivation to introduce theories beyond standard GR. Many modified theories are put forward in literature by different authors, which includes $f(R)$ theory [8]-[10], where R is the Ricci scalar, $f(\tau)$ theory [11]-[13], τ is the torsion scalar, $f(T, B)$ theory [14], where B is a boundary term and T is the trace of stress energy tensor, $f(R, T)$ theory [15, 16], $f(G)$ theory [17], G is the Gauss-Bonnet invariant, $f(R, G)$ theory [18, 19] and many more.

In recent years, $f(Q)$ theory of gravity has been extensively discussed. The $f(Q)$ theory was introduced by Jimenez et al. [20], which is also called symmetric teleparallel gravity and gravity is assigned to non-metricity term Q. It is fitted well with recent cosmological data. The question is: why we need this gravity? is answerable by describing the efficiency of this gravity. As we observe $f(\tau)$ gravity, at a point it is unable to solve coupling problems. Then, $f(Q)$ theory was suggested to check either it is helpful in solving these issues or not. The $f(\tau)$ gravity models face coupling problems when examining perturbations around Friedmann-Lemaitre-Robertson-Walker (FLRW) framework. While $f(Q)$ gravity models seems to be compatible and have ability to solve coupling issues. The main linear perturbation equation for scalar, vector and tensor modes was obtained, displaying specific modifications to the ΛCDM model [21]. For different parameterizations of $f(Q)$ as an explicit function of redshift z, restrictions at the background level have been imposed to examine the expansion rate data from ancient galaxies, SNIa, quasars, gamma ray bursts, Baryonic Acoustic Oscillations (BAO) data, and Cosmic Microwave Background (CMB) data [22]. An extended version of $f(Q)$ gravity is also proposed in literature by coupling Q with T, represented as $f(Q,T)$ theory [23].

An investigation of similar nature has been conducted taking a power-law form of $f(Q)$ model as $f(Q) = Q + \alpha Q^n$ where n can be any positive integer [24]. For this model, the evolution of the growth index of matter perturbations as well as cosmological solutions have been studied. On the other hand, an exponential form of the $f(Q)$ function has just been proposed $f(Q) = Qe^{\frac{\lambda Q_0}{Q}}$, which is demonstrated to have a statistical preference over ΛCDM when the combination of cosmic chronometers, SNIa and BAO data sets is examined [25].

The expansion history of the cosmos in $f(Q)$ gravity receives immediate attention. It will be safe to say that $f(Q)$ gravity is successful in explaining the accelerating expansion of the cosmos at least to the same level of statistic precision of most renowned modified gravities. Many scientists have done research on exploring the nature and background of $f(Q)$ gravity. Mandal et al. [26] explored the energy conditions to examine either their assumed cosmological models are stable or not, and compared the model's parameters with the present values of cosmological parameters in $f(Q)$ gravity. Lu et al. [27] studied symmetric teleparallel gravity in comparison with $f(\tau)$ and $f(R)$ theories of gravity, and established some interesting outcomes. $f(Q)$ gravity also inspires the related bouncing universe model [28] and several modified gravities [29]. Runkla along with Vilson [30], and Gakis et al. [31] investigated the cosmic evolution in symmetric teleparallel theory by reconstructing the scalar non-metricity theories, obtained the field equations and explored their properties. Harko et al.

[32] suggested that symmetric teleparallel gravity can be extended by considering non-minimal coupling between the non-metricity term Q and the matter Lagrangian. In this formalism, they calculated some cosmological angles by assuming power-law and exponential forms of $f(Q)$.

Moreover, exploring symmetric teleparallel gravity is appealing because the field equations are of second order, making them simple to solve. The cosmological implications of the $f(Q)$ theory and its observational constraints were investigated by Ayuso et al. [33]. Kyllep with his collaborators [25] analyzed the matter perturbation in $f(Q)$ gravity through growth index and found its cosmological implications. They worked by assuming power-law function of non-metricity scalar. Under the same background, Hassan et al. [34] investigated static, spherically symmetric traversable wormholes. Barros et al. [35] numerically calculated the linear matter perturbations for two $f(Q)$ models, and checked them working opposite to redshift space distortions data. Lu et al. [36] explored an extension of the symmetric teleparallel gravity by considering a function of the non-metricity invariant Q as the gravitational Lagrangian. Anagnostopoulos et al. [37] found that $f(Q)$ can challenge ΛCDM model and provided the evidence for it. Zhao et al. [38] developed $f(Q)$ theory in a covariant approach where they found suitable non-vanishing affine connection.

In this thesis, we study cosmological implications of two distinct models of $f(Q)$ gravity: First is power-law form $f(Q) = Q + \alpha Q^2$ and second is exponential $f(Q) = Qe^{\frac{\lambda Q_0}{Q}}$.

- **Chapter 2** includes a quick review of applicable primary principles and mathematical formalism, which might be useful to understand research work.

- **Chapter 3** includes background equations for flat FRW space-time in the framework of $f(Q)$ gravity. We characterize the universe by developing some cosmological parameters in terms of redshift parameter. The results are elaborated graphically by constraining the involved model parameters with current astrophysical data. Also, we analyze the matter perturbation of Newtonian gauge for general $f(Q)$ theory.

- The results are concluded in **Chapter 4**.

Chapter 2

Preliminaries

This chapter includes some basic definitions and mathematical formalism that are required to comprehend this thesis. The Greek letters has variation 0,1,2,3 and alphabets has three variations 1,2,3 throughout the thesis.

2.1 Special Theory of Relativity

In special theory of relativity, motion is discussed relative to a fixed point called a frame of reference in which all bodies have inertia to resist any change to their motion (curvature and acceleration is zero). Inertial frame of reference obeys Newton's first law of motion. This theory can be deduced from two fundamental postulates [39]:

- Principle of Relativity: This principle states that no any physical measurement can trace the absolute velocity of an observer, the result of any experiment, performed by an observer do not depend on his speed relative to other observer who are not involved in the experiment.

- Universality of Speed of Light: The speed of light relative to any non-accelerated observer is $c = 3 \times 10^8 ms^{-1}$, regardless of motion of light's source relative to observer.

2.2 General Theory of Relativity

General theory of relativity is the generalization of special relativity. It is a theory of space-time and gravity that was put forward in 1915. Certainly, it is one of the outstanding scientific achievements of all time [40]. General relativity is concerned with both inertial and non-inertial frames of reference. This theory is based on following fundamental principles:

1. General Covariance Principle:

This principle states that, all physical laws are the same for any two physical systems that are moving relatively, which means that laws are independent of the choice of coordinates. This principle helps to resolve the confusion of coordinate system by writing these laws in tensorial form.

2. Equivalence Principle:

   The equivalence principle is one of the foundation of GR. According to it, in the absence of a gravitational field, no local non-gravitational experiment can explain the difference between a freely falling non-rotating system and a uniformly moving system. It implies that inertia and gravity can not be separated.

2.3 Cosmology

Cosmology is the branch of astronomy, which studies the cosmos as a whole including its origin, evolution, behavior, and ultimate destiny. Many philosophers, astrophysicists, and astronomers are attracted to this subject because of numerous findings in it. Cosmology was developed after Einstein's idea of static cosmos. Modern cosmology is based on observational astronomy and fundamental scientific principles that follow from big-bang theory.

2.3.1 Types of Cosmology

There are three types of cosmology:

- **Physical Cosmology** is the study of universe on large scales and its dynamics, and deals with basic questions about its birth and evolution. It also explains important laws of physics that are found to be helpful in recognizing the fundamental facts of the cosmos.

- **Observational Cosmology** describes the chemical composition of cosmos, its density and expansion rate. It began when Hubble in 1929 discovered the expanding cosmos and he described that the universe is not static but experiencing an expanding phase.

- **Theoretical Cosmology** is the study of the evolution and composition of cosmos as a system, developing theories and testing them with experiments and observations [41].

2.4 Accelerating Phenomena of the Universe

The accelerating expansion of cosmos is the phenomena in which the universe is expanding in a way that the recessional velocity of the observer to the distant galaxy is continuously growing with time. The cosmic acceleration was detected by two projects, high-z supernova search team and supernova cosmology project. The surprising result was that celestial objects in the universe are rapidly drifting away from one another. At that time, cosmologists predicted that due to gravitational pull of matter, the velocity at which a distant galaxy recedes from Earth may still decelerate. Finally in 2011, three members of these two groups (Perlmuttar, Riess and Schmidt) were awarded Nobel Prize for this achievement. The rapid expansion of the cosmos is considered to have begun 13.7 billion years ago, when the cosmos entered into DE dominated phase [42]. Accelerating expansion can be described in the framework of GR by a positive cosmological constant, which is comparable to vacuum energy so-called DE.

2.5 Cosmic Components of Dark Regions

Our cosmos has three types of ingredients, ordinary matter, DE and DM. In cosmology, most of the queries are concerned with DE and DM, that are identified

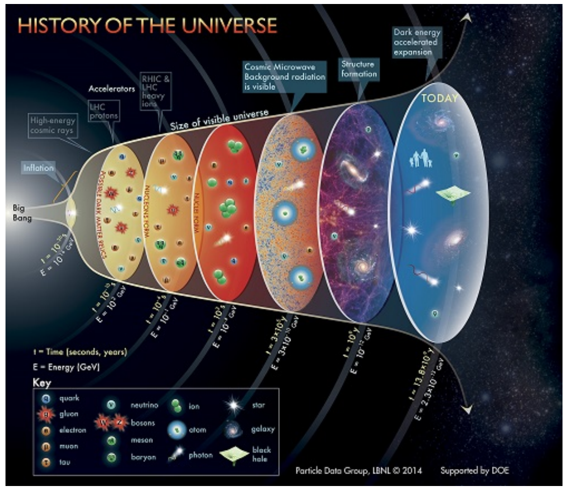

Figure 2.1: Accelerating expansion of the universe [43].

by their gravitational interactions. We can not observe these dark components directly. Many unusual characteristics emerged in the history of universe, providing some cosmic variations and give details about the origin and current state of the universe. It has been noted that our cosmos is not only expanding but experiencing accelerating expansion due to DE [44].

2.5.1 Dark Energy

Observational data accumulated by Riess et al. [2] and Perlmutter et al. [3] is reported that present cosmos has accelerating nature. The source for this late-time cosmic acceleration is DE. It has become center of attraction among all the components of the cosmos due to its unpredictable nature. The word "dark" is attached to this energy because of its mysterious features. Despite the research of many years, its origin has yet to be discovered. For computing DE, many theories have been offered throughout the years, but none of them have survived to satisfy rigorous local testing. Dark energy has negative pressure, which is the main cause of the accelerating cosmic expansion, and act as a counter gravitational force. More is unknown than known about this energy effecting the cosmos on large scale.

2.5.2 Dark Matter

The term “DE" may be somehow confusing because related expression “DM" has been used to refer a pressureless matter (a non-relativistic matter) that interacts with particles of standard matter very weakly. By comparing the dispersion velocities of galaxies in the Coma cluster with observed star mass, Zwicky discovered the existence of DM. Because DM does not transmit the electromagnetic force, gravitational effects on visible matter are used to infer its presence. Dark matter can cluster due to gravitational instability (unlike standard DE), resulting in the formation of local structures in the universe. In fact, DM has been observed to play a major role in the growth of large scale structure such as, galaxies and clusters of galaxies. On There are two categories of DM, baryonic and non-baryonic DM. Baryonic matter contributes 4.2% of total DM. Non-baryonic matter constitutes 22.6% [45].

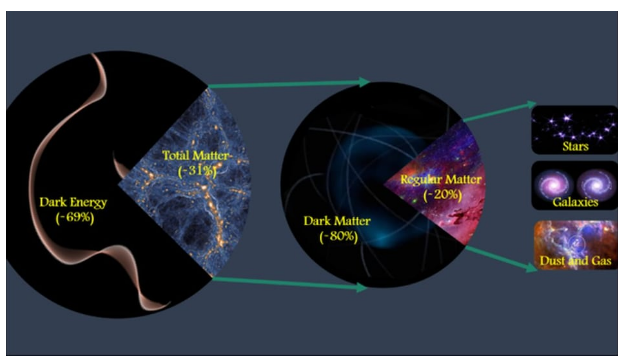

Figure 2.2: Cosmic components of dark regions [46].

2.6 Some Tools to Study Cosmology

This section presented some cosmological parameters that are very efficient to recognize the expanding nature of the universe.

2.6.1 Scale Factor

It gives information about evolution of the cosmos as its size increases with time. The factor $a(t)$ represents expansion, but we do not know how fast the universe is expanding. This issue can be solved by taking derivatives of $a(t)$ with respect to time. The first positive derivative specify that the “universe is expanding". For $\ddot{a}(t) > 0$, the expansion is rapid and positivity of third derivative indicates super acceleration. One of the main features of this parameter is that it can distinguish between isotropic and anisotropic cosmic models. As $a(t)$ remains the same regardless of the spatial directions, it is said to be “isotropic". Bianchi models with different scale factors in different directions are described as “anisotropic".

2.6.2 Hubble Parameter

In 1929, Edwin Hubble stated that “the recessional velocity is proportional to the distance of galaxies from the earth measured by z". It is depicted as

$$v = Hd, \tag{2.1}$$

here v denotes the recessional velocity, d is the distance of galaxy from Earth and H is the proportionality constant (considered as Hubble parameter) and it is expressed as

$$H = \frac{\dot{a}}{a}. \tag{2.2}$$

It represents the rate of expansion. The current value of Hubble parameter is represented by H_0. According to recent observations, the value of H_0 at current time t_0 is $H_0 = 73.8 Km/sec/Mpc$ with 3% uncertainty [47].

2.6.3 Hubble Time

Hubble time is the reciprocal of Hubble constant $\frac{1}{H_0}$. Basically, it is the time that universe is required to expand to its present size, assuming that the Hubble constant has not changed since the big-bang.

2.6.4 Deceleration Parameter

The three phases of the cosmos are described by the deceleration parameter that are accelerating phase $q < 0$, decelerating $q > 0$ and static phase $q = 0$, to narrate the overall nature of cosmic expansion. It is indicated by q, and defined as

$$q = -\frac{a\ddot{a}}{\dot{a}^2} = -1 - \frac{\dot{H}}{H^2}, \tag{2.3}$$

this term is attained by expanding $a(t)$ in Taylor series at the present time t_0.

$$a(t) = a(t_0) + \dot{a}(t_0)[t - t_0] + \frac{1}{2}\ddot{a}(t_0)[t - t_0]^2 ...,$$

dividing this equation by $a(t_0)$ by keeping this in mind that $H_0 = \frac{\dot{a}(t_0}{a(t_0)}$, the above equation is modified to

$$\frac{a(t)}{a(t_0)} = 1 + H_0[t - t_0] - \frac{q_0}{2} H_0^2 [t - t_0]^2.$$

2.6.5 Cosmological Redshift

Based on laboratory experiments on Earth, a specific wavelength is emitted by each element in the periodic table. These photons appear as emission lines or absorption lines in the spectrum of an astronomical object. We can identify the elements that are present inside the object or along the line of sight by analyzing the characteristics of these spectral lines. When astronomers conduct this research, they discovered that most astronomical objects observed spectral lines have all been moved to longer wavelengths, this phenomena is known as cosmological redshift. The cosmological redshift is denoted by z, and formulated as

$$z = \frac{\lambda_{obs} - \lambda_0}{\lambda_0},$$

here λ_{obs} denotes observed wavelength and λ_0 defines emitted/absorbed wavelength. The value of z indicates the distance between relative objects. Cosmological redshift is related to recessional velocity v as $z \approx \frac{v}{c}$, where c is the speed of light. Redshift is associated to expansion factor a describes by the following form

$$1 + z = \frac{1}{a(t)}. \tag{2.4}$$

2.6.6 Equation of State Parameter

In thermodynamics, the physical state of a system is expressed by EoS parameter as it provides relationship between thermodynamical quantities like pressure, energy density and temperature. Mathematically, this relation can be expressed as

$$P = P(\rho, T). \tag{2.5}$$

This is a dimensionless parameter in cosmology, but it has been considered to be a function of time and redshift in some cases. In cosmology, the main role of EoS parameter is that it describes distinct eras of the universe, which are characterized in the following Table.

Eras	EoS parameter
Phantom era	$\omega < -1$
DE-dominated era	$\omega \leq -\frac{1}{3}$
Quintessence era	$-1 < \omega < -\frac{1}{3}$
Stiff-matter era	$\omega = 1$
Radiation-dominated era	$\omega = \frac{1}{3}$
Matter-dominated era	$\omega = 0$

Table 2.1: Distinct cosmic epoch for different ranges of EoS parameter.

2.6.7 Statefinder Pair

Statefinder pair (j, s) is developed using Hubble and deceleration parameters. To distinguish among DE models, many authors have proposed various techniques in the literature. The discrimination is required between these proposed models in order to determine which one explains more precisely the current state of the cosmos. For this purpose, Sahni et al. [7] introduced a pair of dimensionless parameters. Jerk parameter can be determined through following mathematical formula

$$j = \frac{\dddot{a}(t)}{a(t)H^3(t)} = \frac{\ddot{H}(t)}{H^3(t)} + 3\frac{\dot{H}(t)}{H^2(t)} + 1, \tag{2.6}$$

while in terms of q, j reads as

$$j = \frac{\ddot{H}(t)}{H^3(t)} - 3q - 2. \tag{2.7}$$

Snap parameter has following mathematical formula

$$s = \frac{j-1}{3(q-\frac{1}{3})}. \tag{2.8}$$

Because of their dependence on scale factor, these parameters are known as geometrical diagnostic. Based on these two cosmological parameters, we can define some well-known regions:

- $(j, s) = (1, 1)$ shows CDM model,
- $(j, s) = (1, 0)$ indicates ΛCDM model,
- $j < 1$ and $s > 0$ represents the quintessence and phantom regions.
- $j > 1$and $s < 0$ indicates Chaplygin gas behavior.

2.6.8 $Om(z)$ Diagnostic

The $Om(z)$ diagnostic is another way to describe different eras of cosmos. The $Om(z)$ diagnostic in term of z function is described as

$$Om(z) = \frac{\frac{H^2}{H_0} - 1}{z^3 - 1}. \tag{2.9}$$

The positive slope of the curve shows phantom phase and $Om(z) < 0$ indicates the quintessence region.

2.6.9 Square Speed of Sound

The square speed of sound is a significant quantity to determine the stability of the underlying model. It is denoted by v_s^2 and is calculated by following formula

$$v_s^2 = \frac{dp}{d\rho}. \tag{2.10}$$

If $v_s^2 > 0$, the model will be stable otherwise unstable.

2.7 Einstein Field Equations in General Relativity

Einstein field equations are the fundamental equations in GTR, that are developed by the following action

$$S = \int \sqrt{-g}(R + L_m)d^4x, \tag{2.11}$$

here L_m is the matter Lagrangian, g be the determinant of the metric tensor $g_{\mu\nu}$. On varying this action with respect to $g_{\mu\nu}$, we obtain the second order partial deferential equations which connect the geometry of space-time to the distribution of matter within it. The general equations can be described as

$$G_{\mu\nu} = \kappa T_{\mu\nu}, \tag{2.12}$$

here $G_{\mu\nu}$ is the Einstein tensor which can be defined as

$$G_{\mu\nu} = R_{\mu\nu} - \frac{1}{2}Rg_{\mu\nu}, \tag{2.13}$$

here $R_{\mu\nu}$ is the Ricci tensor and can be defined as

$$R_{\mu\nu} = -\Gamma^{\alpha}_{\mu\nu,\alpha} + \Gamma^{\alpha}_{\mu\alpha,\nu} + \Gamma^{\rho}_{\mu\alpha}\Gamma^{\alpha}_{\nu\rho} - \Gamma^{\alpha}_{\mu\nu}\Gamma^{\rho}_{\alpha\rho}, \tag{2.14}$$

here $\Gamma^{\mu}_{\nu\alpha} = \frac{1}{2}g^{\sigma\mu}(g_{\nu\sigma,\alpha} + g_{\alpha\sigma,\nu} - g_{\nu\alpha,\sigma})$, be the Christoffel symbol. The metric form of stress-energy tensor is described as

$$T_{\mu\nu} = \begin{pmatrix} T_{00} & T_{01} & T_{02} & T_{03} \\ T_{10} & T_{11} & T_{12} & T_{13} \\ T_{20} & T_{21} & T_{22} & T_{23} \\ T_{30} & T_{31} & T_{32} & T_{33} \end{pmatrix} \tag{2.15}$$

here

- T_{00} specify energy density.
- T_{11}, T_{22} and T_{33} represent stress or pressure.
- Upper part of diagonal describe energy flux.
- Lower part of diagonal illustrate momentum density.

2.8 Perfect Fluid

A fluid is a substance that deforms continuously under shear stress, regardless of the magnitude of stress. While perfect fluid (also called an ideal fluid) is described by density and isotropic pressure, having zero viscosity as well as zero heat conduction. The perfect fluid is expressed by the following equation

$$T_{\mu\nu} = (\rho + p)u_\mu u_\nu - p g_{\mu\nu}, \tag{2.16}$$

here u_μ be the four-velocity component and the normalization condition $u^\mu u_\nu = -1$. The four-velocity component is mathematically defined as $u_\mu = \frac{1}{\sqrt{g_{tt}}}(1,0,0,0)$ for $(+,-,-,-)$ signature and $u_\mu = \frac{1}{\sqrt{-g_{tt}}}(1,0,0,0)$ for $(-,+,+,+)$ signature, where g_{tt} is the time component of metric tensor.

2.9 Friedmann Robertson-Walker Metric

The cosmological theory requires that there are no alternative points (homogeneities: invariance under spatial translations) and no ideal paths (isotropy: invariance under spatial rotations) in 3-dimensional space-time. The geometry of space-time is still permitted to focus on time. The metric of the space-time is highly constrained by these assumptions. In 1922, Friedmann established a mathematical model of universe and he observed its expanding nature for the first time. Later in 1935, Roberston and Walker modified this model, which is in agreement with cosmological principle. The combined FRW model describes the observed nature of cosmos. In spherical polar coordinates $x^i = (t, r, \theta, \phi)$, the line-element for FRW model is described as

$$ds^2 = -dt^2 + a^2(t)\left(\frac{dr^2}{1 - Kr^2} + r^2(d\theta^2 + \sin^2\theta d\phi^2)\right), \tag{2.17}$$

here K is the curvature parameter and r, θ, ϕ are the co-moving coordinates. The curvature parameter has three different values described in Table **2.2**:

Curvature Parameter	Type of universe	Geometry	Circumference of circle	Angles
$K = 0$	Flat	Flat	$= 2\pi r$	$= 180°$
$K = -1$	Open	Hyperbolic	$> 2\pi r$	$< 180°$
$K = 1$	Closed	Spherical	$< 2\pi r$	$> 180°$

Table 2.2: Possible geometries of the universe.

2.10 Modified Theories of Gravity

To find compatible candidate of DE and to resolve the issues of late-time acceleration and early-time inflation, several DE proposals including the modification of geometry or modification of matter in Einstein-Hilbert action are presented. In past decade, modification of GR at large scale was suggested by many theoretical and observational features. In curved space-time and low energy limit of string theory, quantum field theories are suggested as the effective Lagrangian, carrying higher order curvature invariants. Furthermore, many researchers think that the solar system experiments are insufficient to prove that GR is the only stable theory. Despite of having achieved little success in explaining cosmic acceleration so far, research in modified gravity is essential because they produce logical, consistent alternatives to GR and may address several existing issues. A lot of research on modified gravity theories have been conducted in the last two decades to discover and explain the profile of universe. In past, a family of modified gravity theories has been developed that extends GR in some way, for example, $f(R)$ theory [48], $f(\tau)$ theory, $f(R,T)$theory, $f(G)$ theory, $f(R,G)$ theory. In this thesis, we will focus on $f(Q)$ theory.

2.11 $f(Q)$ Theory of Gravity

In recent years, $f(Q)$ and its extended theories of gravity have been extensively discussed. $f(Q)$ theory is also called symmetric teleparallel gravity, where one thinks of vanishing curvature and torsion, and the non-metricity term Q describes the gravitational interaction. Some other interesting cases can be imagined: for example, a geometry where torsion carries part of the gravitational force and non-metricity term is not working. Furthermore, by considering the affine connection, the metric-affine geometry is specified. We know that the metric tensor $g_{\mu\nu}$, is generalized by gravitational potential, which describes the distances, angles and volumes, while the affine connection accounts for covariant derivatives and parallel transport. In differential geometry [49], the general affine connection is described as

$$\Gamma^{\lambda}{}_{\mu\nu} = \{^{\lambda}{}_{\mu\nu}\} + K^{\lambda}{}_{\mu\nu} + L^{\lambda}{}_{\mu\nu}, \tag{2.18}$$

where Levi-Civita connection of the metric is defined as

$$\{^{\lambda}{}_{\mu\nu}\} \equiv \frac{1}{2} g^{\lambda\beta}(\partial_{\mu} g_{\beta\nu} + \partial_{\nu} g_{\beta\mu} - \partial_{\beta} g_{\mu\nu}), \tag{2.19}$$

the contortion tensor is defined as

$$K^{\lambda}{}_{\mu\nu} = \frac{1}{2}\tau^{\lambda}{}_{\mu\nu} + \tau_{(\mu}{}^{\lambda}{}_{\nu)}, \tag{2.20}$$

with torsion tensor $\tau^{\lambda}{}_{\mu\nu} = 2\Gamma^{\lambda}{}_{\mu\nu}$, the disformation tensor $L^{\lambda}_{\mu\nu}$, can be expressed in terms of non-metricity tensor as

$$L^{\lambda}{}_{\mu\nu} = \frac{1}{2} g^{\lambda\beta}(-Q_{\mu\beta\nu} - Q_{\nu\beta\mu} + Q_{\beta\mu\nu}). \tag{2.21}$$

Here the non-metricity tensor $Q_{\gamma\mu\nu}$, can be represented as

$$Q_{\gamma\mu\nu} = -\frac{\partial g_{\mu\nu}}{\partial x^{\gamma}} + g_{\nu\lambda}\Gamma^{\lambda}{}_{\mu\gamma} + g_{\lambda\mu}\Gamma^{\lambda}{}_{\nu\gamma}. \tag{2.22}$$

Recently, $f(Q)$ gravity has introduced various interesting results at solar system, galactic and cosmological scales. It is the most simplest modification of GR in which $f(Q)$ is an arbitrary function of non-metricity scalar. The action of $f(Q)$ is described as

$$S = \int (-\frac{1}{2}f(Q) + L_m)\sqrt{-g}d^4x. \tag{2.23}$$

In the flat space the action (2.23) is equivalent to GR when $f = 0$, since the symmetric teleparallel action is reconstructed. Therefore any modification to GR may be observed for $f \neq 0$. The non-metricity tensor and its traces can be written as

$$Q_{\gamma\mu\nu} = \nabla_\gamma g_{\mu\nu}, \tag{2.24}$$

$$Q_\gamma = Q_\gamma{}^\mu{}_\mu, \quad \tilde{Q}_\gamma = Q^\mu{}_{\gamma\mu}. \tag{2.25}$$

Furthermore, the superpotential as a function of non-metricity tensor is formulated as

$$P^\gamma_{\mu\nu} = \frac{1}{4}(-Q^\gamma_{\mu\nu} + 2Q_\mu{}^\lambda{}_\nu - Q^\gamma g_{\mu\nu} - \tilde{Q}^\gamma g_{\mu\nu} - \delta^\gamma{}_{(\gamma}Q_{\nu)}), \tag{2.26}$$

the non-metricity scalar is defined as

$$Q = -Q_{\gamma\mu\nu}P^{\gamma\mu\nu}. \tag{2.27}$$

The field equations can be obtained by varying the action with respect to metric tensor as given below

$$\frac{2}{\sqrt{-g}}\nabla_\gamma(\sqrt{-g}f_Q P^\gamma_{\mu\nu}) + \frac{1}{2}g_{\mu\nu}f + f_Q(P_{\mu\gamma i}Q_\nu{}^{\gamma i} - 2Q_{\gamma i\mu}P_{\gamma i}{}^\nu) = -T_{\mu\nu}, \tag{2.28}$$

where $f_Q = \frac{df}{dQ}$. We can also take the variation of action with respect to the connection, which provide following equations

$$\nabla_\mu\nabla_\gamma(\sqrt{-g}f_Q P^\gamma_{\mu\nu}) = 0. \tag{2.29}$$

By choosing any compatible line-element, we can generate corresponding field equations.

2.12 Fixed Points

There is another approach to examine the stability of model, which is to calculate fixed points of the system. Here is an algorithm to describe how we can calculate fixed points:

- By using field equations, calculate a system of equations, it follows that

$$\begin{aligned} \frac{dh_1}{dX} &= K_1(h_1, h_2, h_3 \cdots, h_n), \\ \frac{dh_2}{dX} &= K_2(h_1, h_2, h_3 \cdots, h_n), \\ &\vdots \\ \frac{dh_n}{dX} &= K_3(h_1, h_2, h_3 \cdots, h_n), \end{aligned}$$

  where $h_1, h_2, h_3..., h_n$ are dimensionless variables and $X = \ln a$.

- Calculate the fixed points by taking

$$\frac{dh_1}{dX} = 0, \quad \frac{dh_2}{dX} = 0, \ldots, \frac{dh_n}{dX} = 0. \tag{2.30}$$

- Form a Jacobian matrix and calculate its eigenvalues to characterize the fixed points. The Jacobian matrix is denoted by J and can be defined as

$$J = \begin{pmatrix} \frac{\partial K_1}{\partial h_1} & \frac{\partial K_1}{\partial h_2} & \cdots & \frac{\partial K_1}{\partial h_n} \\ \frac{\partial K_2}{\partial h_1} & \frac{\partial K_2}{\partial h_2} & \cdots & \frac{\partial K_2}{\partial h_n} \\ \frac{\partial K_3}{\partial h_1} & \frac{\partial K_3}{\partial h_2} & \cdots & \frac{\partial K_3}{\partial h_n} \\ \vdots & & & \\ \frac{\partial K_n}{\partial h_1} & \frac{\partial K_n}{\partial h_2} & \cdots & \frac{\partial K_n}{\partial h_n} \end{pmatrix} \tag{2.31}$$

2.12.1 Classification of Fixed Points

A fixed point is a point that does not change when a system of differential equations or mapping is applied on it. For example, a point y_0 will be the fixed point of a function $f(y)$, satisfying $f(y_0) = y_0$. fixed points are categorized into two types, hyperbolic (eigenvalues are real points) and non-hyperbolic points (eigenvalues are imaginary points) Hyperbolic points are further categorized into three types

- For eigenvalues with negative real parts, the hyperbolic point is known as attractor.
- If eigenvalues consist of positive real part then hyperbolic point will be oscillator or source.
- If eigenvalues have opposite signs then hyperbolic point is referred to a saddle point.

2.13 Cosmological Perturbation Theory

The standard model of hot big-bang cosmology is FRW model, which is spatially homogeneous and isotropic. This successfully depicts the average expansion of the universe on large scales according to Einstein's GR. However, a homogenous model can not explain the complexities of matter and energy distribution in our observed cosmos, where stars and galaxies form clusters and super-clusters across a wide range of scales. Large scale inhomogeneous structures of the universe, including galaxies and clusters of galaxies, are usually assumed to have originated as a result of the growth of density fluctuations whose amplitudes had been very small in the early universe. However, there exist few exact solutions of GR that include spatially inhomogeneous and anisotropic matter and geometry. Thus, we have used a perturbative approach starting from the spatially homogeneous and isotropic FRW model as a background solution with simple properties within which we can examine the complexity of inhomogeneous perturbations order by order. In perturbed cosmos, there must be a coordinate system, whose metric can be written as

$$g_{\mu\nu} = \bar{g}_{\mu\nu} + \delta g_{\mu\nu}, \tag{2.32}$$

where $\bar{g}_{\mu\nu}$ is the metric of the background space-time and $\delta g_{\mu\nu}$ be the perturbation part, one must select between them because both are not similar. In GR, there is no preferred choice of coordinates. By considering a set of coordinates in inhomogeneous cosmos, which will be characterized by a FRW model with perturbations is equivalent to assigning a mapping between inhomogeneous universe space-time points and the homogeneous background model. The freedom in this choice is the gauge freedom. The first gauge employed in cosmological perturbation was the synchronous gauge (introduced by Lifshitz in 1946) and can be used in both scalar and vector perturbation [50]. It can be defined by the requirement $B = 0$ as

$$ds^2 = a^2[-dt^2 + ((1 - 2\Psi)\delta_{ij} + 2E_{ij})dx^i dx^j], \tag{2.33}$$

during this gauge transformation, we will approach to Newtonian gauge which is known as longitudinal gauge or Poisson gauge. Thus scalar perturbation of metric in Newtonian gauge ($B = E = 0$), where B is magnetic induction vector and E is electric field intensities, including Bardeen potentials $\Phi(t, \vec{x})$ and $\Psi(t, \vec{x})$ can be written as

$$ds^2 = a^2[-(1 + 2\Phi)dt^2 + (1 - 2\Psi)d\vec{x}^2]. \tag{2.34}$$

The theory of cosmological perturbation predicts that perturbations are appropriately small. For example, the energy density contrast $\delta = \frac{\delta\rho}{\rho}$. To explain it using cosmological perturbation theory, one needs to fulfill $|\delta(\mathbf{x}) \ll 1|$. This might be true in the early cosmos without any smoothing, however, as galaxies evolve, we will definitely need to smooth on a scale carrying many galaxies. At a given point, the smoothed quantity is the average of original quantity within a comoving sphere of radius aR. Smoothing is frequently required to deal with cosmological perturbations, and it raises a number of challenges. One must be careful about which quantities are being smoothed. In practice, smoothing is usually only utilized for the metric perturbations, the energy momentum tensor, and scalar fields. In terms of Fourier components, smoothing on a scale R, corresponds to dropping components with wavenumber less than $k = 1/R$. With this in mind, the smoothing scale is commonly referred to $1/k$ rather than R.

During the super-horizon era $k \ll aH$, the separate universe concept relates to the behavior of universe after smoothing on a described comoving scale k^{-1}. It may be described more accurately by a set of assumptions. The first assumption is that: spatial gradients are negligible, at least of order k/a. This assumption will cause the universe to evolve in a homogeneous manner at every location. The second supposition holds that the cosmos is locally isotropic at every location. According to both assumptions, the smoothed universe at each point evolves like some unperturbed (homogeneous and isotropic) universe throughout the super-horizon regime.

Chapter 3

Cosmological Evolution in $f(Q)$ Gravity

3.1 Overview of $f(Q)$ Gravity

The action of $f(Q)$ gravity is given in Eq. (2.23). By varying the action with respect to metric tensor, the modified Einstein field equations are given in Eq. (2.28). The non-metricity tensor and its traces are defined in Eq. (2.24). The central character, which is the non-metricity scalar is described in Eq. (2.27). In this theory, the energy conservation equation has the following form

$$\nabla^{\mu} T_{\mu\nu} = (\dot{S} + 6HS), \tag{3.1}$$

here $S = 2(H\dot{f}_Q + \dot{H} f_Q)$. Assume that universe is described by the FRW line-element, which is isotropic, homogeneous and spatially flat

$$ds^2 = -dt^2 + a^2(t)(d\vec{x}^2), \tag{3.2}$$

where $\vec{x}$ be the three dimensional space. The matter part of cosmos is filled with perfect fluid, the energy momentum tensor for perfect fluid is written in Eq. (2.16).

The Friedmann and Raychaudhuri equations will be derived by using Einstein equations given in (2.28) as follows

$$\rho = -6f_Q H^2 + \frac{f}{2}, \tag{3.3}$$

$$p = 2\dot{H} f(Q) + 6f(Q)H^2 + 2\dot{f}_Q H - \frac{f}{2}, \tag{3.4}$$

here $\dot{f}_Q = \frac{df_Q}{dt}$, $\rho = \rho_m + \rho_r$, and ρ_m, ρ_r are the energy densities of matter and radiation, respectively. The condition $f(Q) = Q$, where $Q = 6H^2$ for FRW metric, is efficient enough in fitting with the current cosmological data. The conservation equation (3.1) turns out to be

$$\dot{\rho} + 3H(\rho + p) = 2\ddot{f}_Q H + 4\dot{H}\dot{f}_Q + 2f_Q \ddot{H} + 6H(2\dot{f}_Q H + 2f_Q \dot{H}). \tag{3.5}$$

In next section, we will complete the dynamical analysis considering power-law $f(Q)$ model.

3.1.1 $f(Q) = Q + \alpha Q^2$

Now we will use power-law form of $f(Q)$ model, i.e., $f(Q) = Q + \alpha Q^2$, where α is an arbitrary constant [24]. We will analyze the behavior of cosmological model at background and perturbation level. By using this model, the Friedmann, Raychaudhuri and conservation equations take the following form

$$\begin{aligned} \rho &= -6H^2 - 54\alpha H^4, && (3.6) \\ p &= 2\dot{H} + 3H^2 + 36\alpha H^4 + 48\alpha H^2 \dot{H}, && (3.7) \\ \dot{\rho} + 3H(\rho + p) &= 144\alpha H\dot{H}^2 + 72\alpha \ddot{H} H^2 - 432\alpha H^3 \dot{H} + 2\ddot{H} - 12H\dot{H}. && (3.8) \end{aligned}$$

Here, we assume that universe is filled with dust and radiation fluids with EoS $p_m = 0$ and $p = \frac{1}{3}\rho_r$, respectively. We can see from above system of equations that for $\alpha = 0$, we move towards original theory. Suppose that matter and radiation are not interacting with each other, their combination will not be conserved in general and the universe has a lower radiation abundance than dust. Therefore, we assume that radiation part of cosmos is conserved and all non-conservation factors in (3.8) are carried by dust.

To simplify the results, we use dimensionless parameters to observe cosmic consequences. The following dimensionless variables are being introduced

$$\tau = H_0 t, \quad H = H_0 h, \quad \bar{\rho}_i = \frac{\rho_i}{6H_0^2}, \tag{3.9}$$

here $i = m, r$ corresponds to dust and radiation, respectively and current value of Hubble parameter is denoted by H_0. The Friedmann Eq. (3.6), Raychaudhuri Eq. (3.7) and conservation Eq. (3.8) in dimensionless form will be as, respectively

$$\begin{aligned}
\bar{\rho_m} + \bar{\rho_r} &= \frac{1}{2}h^2 + 2\alpha H_0^2 h^2, && (3.10)\\
\frac{1}{2}h^2 + \frac{1}{3}\frac{\dot{h}}{H_0^2} &= -\bar{\rho_r} - 3\alpha h^2(3H_0^2h^2 + 4\dot{h}), && (3.11)\\
\bar{\rho_r}' + 4h\bar{\rho_r} &= 0, && (3.12)\\
\frac{1}{H_0}\bar{\rho_m}' + 3h\bar{\rho_m} &= 24\alpha\frac{h}{H_0^2}\dot{h}^2 + 12\alpha\frac{h^2}{H_0}\ddot{h} - 72\alpha h^3\dot{h} + \frac{\ddot{h}}{3H_0^3} - \frac{2h\dot{h}}{H_0^2}, && (3.13)
\end{aligned}$$

here prime indicates derivative with respect to conformal time τ. Form Eq. (3.12), we can find the evolution of radiation density abundance as follows

$$\bar{\rho_r} = \frac{\Omega_{r0}}{a^4}, \tag{3.14}$$

here $\Omega_{r0} = 5.3 \times 10^{-5}$ be the present radiation abundance.

To compare observational data with cosmological data, redshift parameter is efficient enough to use, defined in Eq. (2.4). We will rewrite Eqs. (3.10) and (3.11) in redshift coordinate as under

$$\begin{aligned}
2\Omega_m(1+z)^4 &+ 2\Omega_{r0}(1+z)^2 - 4\alpha h^2(1+z)^{-2} = (1+z)^2h^2, && (3.15)\\
\frac{1}{2}h^2 - \frac{2}{3}(1+z)hh' &= -\Omega_{r0}(1+z)^4 - 9\alpha h^4 + 24h^3h^{'}(1+z), && (3.16)
\end{aligned}$$

here prime stands for the derivative with respect to z and Ω_m is matter density abundance. Equation (3.13) in redshift coordinate can be written as follows

$$\begin{aligned}
(1+z)\Omega'_m + 3\Omega_m &= \frac{h''}{h} + 24\alpha\frac{h'^2}{h^2} - 72(1+z)h' - 2(1+z)\frac{h'}{h^2}\\
&+ (1+z)^2\frac{h''}{h^2} + 12\alpha(1+z)^2. && (3.17)
\end{aligned}$$

To find fractional densities at present time, we will use $h(z=0) = 1$. Therefore, we get following expression from Eqs. (3.10) and (3.11)

$$\Omega_{m0} + \Omega_{r0} = \frac{5}{2}, \tag{3.18}$$

where $\Omega_{m0} = 0.305$, be the current value of dust fluid abundance.

Deceleration parameter is defined in Eq. (2.3), in dimensionless coordinates, it takes the following form

$$q = (1+z)\frac{h'}{h}, \tag{3.19}$$

where dimensionless Hubble parameter can be achieved from Eq. (3.15) as under

$$h^2 = \frac{2\Omega_{m0}(1+z)^3 + 2\Omega_{r0}(1+z)^4}{1+4\alpha}. \tag{3.20}$$

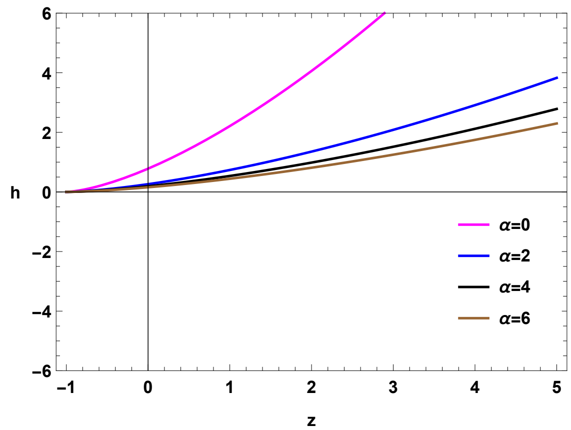

Figure 3.1: h versus z for different values of α.

In Fig. **3.1**, we observe the behavior of calculated dimensionless Hubble parameter as a function of z, which is found to be physical. The graph is showing positively decreasing behavior from past to future for all choosen values of model parameter α. At low redshift, we observe less cosmological evolution, while at higher z, there is a significant impact of parameter on cosmic expansion. All the trajectories are converging to $h \to 0$ as we are approaching to future regime, which is representing that size of the universe a, must be approaching to a specific value. Moreover, for large values of α, we analyze less Hubble expansion, which results in large size of universe.

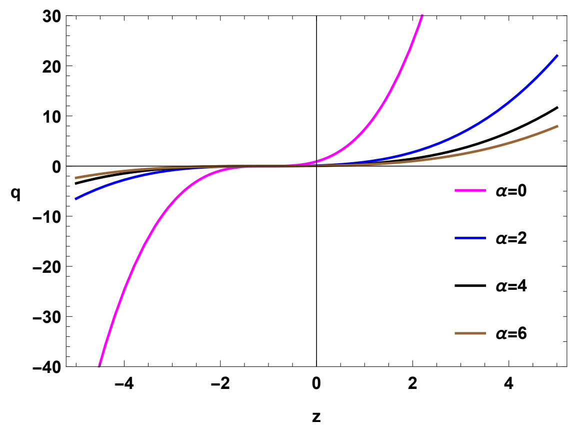

Figure 3.2: q as a function of z for different values of α.

In Fig. **3.2**, we depict the behavior of q versus z. In this graph, a phase transition from deceleration to acceleration is being observed from past to future epoch, respectively for all positive values of α. An opposite trend in q is being noticed for negative values of α. The obtained solution of q is physical and consistent with recent observations.

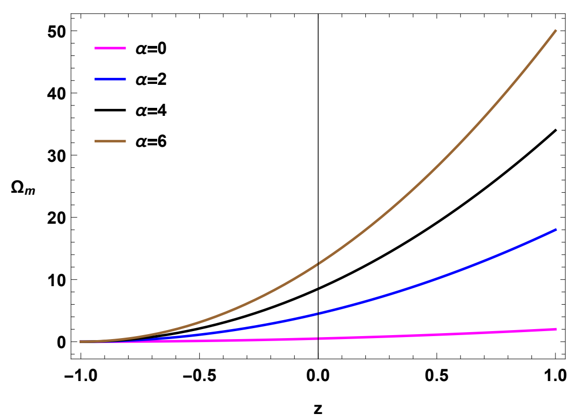

Figure 3.3: Dust abundance versus redshift.

In Fig. **3.3**, we examine the graphical behavior of dust abundance. The expression of Ω_m can be obtained from $\Omega_m = \frac{\bar{\rho}_m a^2}{h^2}$, where h^2 is written in Eq. (3.20)

$$\Omega_m = \frac{\Omega_{m0}(1+4\alpha)}{2\Omega_{m0}(1+z)^8 + 2\Omega_{r0}(1+z)^9}.$$

In this plot, we can see that trajectories are showing decreasing behavior from past to future for all positive values of model parameter α. Moreover, the curves are converging to zero in future, supporting the assumption of dust case.

3.2 Dynamical System Analysis

A powerful and elegant technique to examine the cosmic dynamics is the changing of cosmological equations into a dynamical system. It can be used to analyze the stability of a system and to examine the variety of cosmological models. Dynamical system analysis will help to improve our knowledge of cosmic evolution. Describing the following density abundance.

$$\Omega_i = \frac{\bar{\rho}_i a^2}{h^2}, \quad \Omega_h = \frac{h^2}{a^2}, \tag{3.21}$$

the dynamical variable Ω_h is the density abundance of curvature. By using above parameters in Eq. (3.10), we get the following equation

$$\Omega_m + \Omega_r - \frac{1}{2}a^2\Omega_h^{-1} = 2a^2. \tag{3.22}$$

By using the above independent variables Ω_m, Ω_r and Ω_h, we can derive following dynamical equations

$$\begin{aligned} \Omega_m^{'} &= \Omega_{m0}(-2 - 2(\frac{12\alpha}{4\alpha+1})(-\Omega_{m0} - 2\Omega_{r0} + 2 + 3\alpha) \\ &+ \Omega_{h_0}(2\alpha(\frac{1}{4\alpha+1})(-\Omega_{m0} - 2\Omega_{r0} + 2 + 3\alpha))), \qquad (3.23) \\ \Omega_r^{'} &= \Omega_{r0}((-2 - \frac{12\alpha}{4\alpha+1})(-\Omega_{m0} - 2\Omega_{r0} + 2 + 3\alpha)), \qquad (3.24) \\ \Omega_h^{'} &= \Omega_{h0}((\frac{24\alpha}{4\alpha+1})(-\Omega_{m0} - 2\Omega_{r0} + 2 + 3\alpha) - 2), \qquad (3.25) \end{aligned}$$

here prime refers to the derivative with respect to $\ln a$. Now the effective EoS $\omega_{eff} = \frac{p}{\rho}$, for this model will be $\omega_{eff} = -1 - \frac{2H^{'}}{3H^2}$, while in dimensionless variables, it will be as follows

$$\omega_{eff} = -1 - \frac{2h^{'}}{3h^2} = -1 - \left(\frac{24\alpha}{4\alpha+1}(-\Omega_{m0} - 2\Omega_{r0} - 3\alpha + 2)\right). \tag{3.26}$$

3.2.1 Radiation Fixed Point (P_r):

The fixed point of the dynamical system Eqs. $(29) - (31)$ is

$$P_r = (\Omega_m, \Omega_r, \Omega_h) = (0, 1, 0).$$

ES The point $(0, 1, 0)$ corresponds to the radiation dominated universe $(\omega_{eff} = \frac{1}{3})$, In this case, the eigenvalues are $(-1, 4, 0)$, showing that radiation fixed point is saddle.

3.2.2 Dust Fixed Point (P_m):

$$P_m = (\Omega_m, \Omega_r, \Omega_h) = (1, 0, 0).$$

The point $(1, 0, 0)$ corresponds to the matter dominated universe $\omega_{eff} = 0$. In this case, the eigenvalues associated to the given fixed points are $(-1, -3, 0)$, indicating that dust fixed point is also saddle.

3.2.3 $Om(z)$ and Statefinder Diagnostic

The jerk and snap parameters along with $Om(z)$ parameter are defined in Eqs.(2.7), (2.8) and (2.9), respectively. $Om(z)$ parameter in terms of z can be calculated by using the expression of dimensionless Hubble parameter h^2, which is derived from Eq. (3.15). In Fig. **3.4**, we observe the behavior of $Om(z)$ parameter graphically. In this plot, trajectories are showing positive slope in future, which tends to the phantom era. While in the past, trajectories are transiting from quintessence to phantom region.

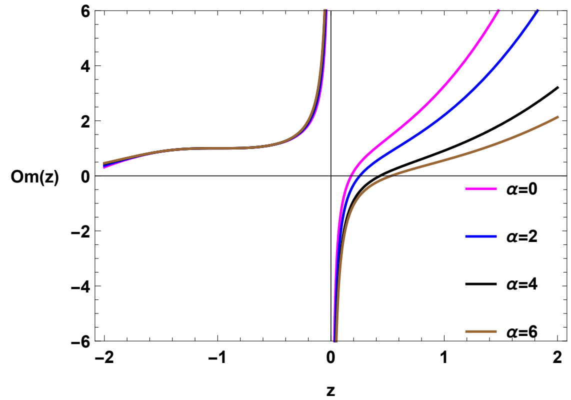

Figure 3.4: Plot of $Om(z)$ diagnostic versus z.

In dimensionless coordinates, the jerk is read as

$$j = \frac{\ddot{h}}{h^3} - 3((1+z)\frac{h'}{h}) - 2, \tag{3.27}$$

here prime indicates the derivative with respect to z.

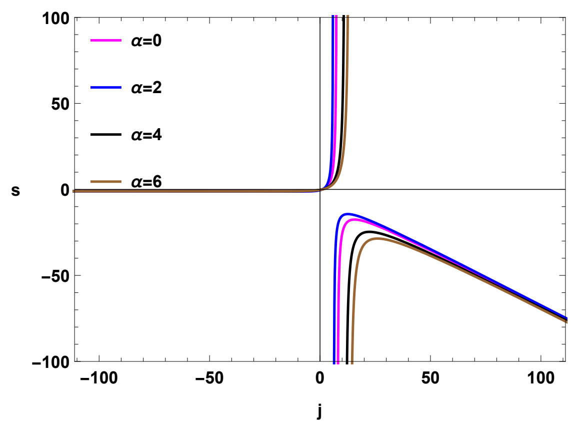

Figure 3.5: Plot of (j, s) by varying values of α.

In Fig. **3.5**, parametric plot of $j - s$ pair has been shown. From this plot, we can see that the considered model is exhibiting the Chaplygin gas behavior as parameters lie in the allowed region $j > 1,\ s < 0$.

3.2.4 Square Speed of Sound

To analyze the stability of model, we use square speed of sound whose expression is given in Eq. (2.10). For underlying model, this expression can be developed using the expressions of pressure and energy density derived from (3.6) and (3.7).

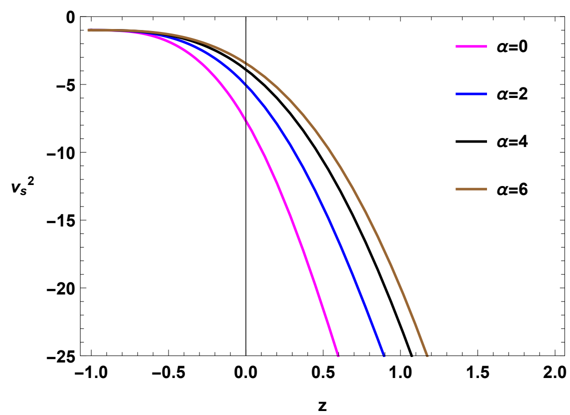

Figure 3.6: Plot of square sound speed versus z for different values of α.

Figure **3.6** is showing that the model is unstable as $v_s^2 < 0$ for all values of α.

3.3 Matter Perturbations

The perturbed line-element in Newtonian gauge is defined in Eq. (2.32). Under this gauge, Φ and Ψ are gauge invariant variables and equation will reduce to FRW in the absence of these variables. In classical cosmological models, these potentials are equivalent during the development of structure. This is no longer the case when modifications in gravitational interaction are considered. The non-metricity scalar for newtonian gauge can be derived from Eq. (2.27). So, by neglecting higher powers of scale factor, we will get expression for Q corresponding to (2.32) as

$$\begin{aligned} Q &= \dot{\Phi}(-6a^2H - 6aH - 90) - \nabla\Phi(18a^2H - \frac{3}{2}H - 15) + 6H^2 \\ &+ \Phi(15H + 6H^2), \end{aligned} \tag{3.28}$$

by assuming $\Phi = 0$, we will get $Q = 6H^2$, which is for FRW line-element. The scalar perturbation of energy momentum tensor can be expressed as

$$\begin{aligned} \delta T^0_0 &= -\delta\rho \equiv -\rho\delta, \\ \delta T^0_i &= (1+\omega)\rho\partial_i\nu, \quad \delta T^i_j = \delta^i_j \delta p, \end{aligned} \tag{3.29}$$

where ν is the scalar mode of velocity perturbation. By assuming $\omega = 0$, we will deal with unperturbed matter content of cosmos, which is dust. The first order perturbation $(i \neq j)$ of Einstein field equations can be obtained for $\Psi = \Phi$. The $(00),\ (0i),\ (ii)$ components of the field equations will be

$$\begin{aligned} a^2\rho\delta_m &+ 4(k^2 + 3H^2)\Phi + 4a^2\acute{f}\bigg(\dot{\Phi}(3H - 6a^2H - 90) + \Phi(15 + 6H^2) \\ &+ k^2\Phi(18a^2H + \frac{3}{2}H - 15)\bigg) = 0, \end{aligned} \tag{3.30}$$

$$\rho\theta - 4\frac{k^2}{a^2}(\dot{\Phi} + H\Phi) = 0, \tag{3.31}$$

$$\begin{aligned} \ddot{\Phi} &+ (\dot{H} + H^2)\Phi + 3H\dot{\Phi} + a^2\acute{f}\bigg(\dot{\Phi}(3H - 6a^2H - 90) + \Phi(15 + 6H^2) \\ &+ k^2\Phi(18a^2H + \frac{3}{2}H - 15)\bigg) = \frac{a^2\delta p}{4}. \end{aligned} \tag{3.32}$$

We will use Fourier transformation to obtain above perturbed fields and $\theta = -k^2\nu$. The Fourier transformed first order perturbations of conservation equations are as follows

$$
\begin{aligned}
a^4\rho\delta\dot{\delta} &+ 3a^4H\delta P + a^4[\dot{\rho}\delta + \rho(3H\delta + \theta - 3\dot{\Phi})] + 4a^2\acute{f}\bigg(\ddot{\Phi}(-6a^2H - 6aH - 90)\\
&+ \dot{\Phi}(-12Ha^2 - 6aH^2 - 6a\dot{H} + 15H + 6H^2) + k^2\dot{\Phi}(18a^H - \frac{3}{2}H - 15)\\
&+ \Phi((18a^2\dot{H} - \frac{3}{2}\dot{H})K^2 + 15\dot{H})\bigg) + 24f''H^2\bigg(\dot{\Phi}(-6a^2H - 6Ha - 90)\\
&+ k^2\Phi(18a^2H - \frac{3}{2}H - 15) + \Phi(15H + 6H^2)\bigg) = 0, \qquad (3.33)\\
\dot{\rho}\theta &+ \rho(4H\theta - k^2\Phi + \dot{\theta}) - k^2\delta p - 4\frac{1}{a^2}\acute{f}\bigg(\dot{\Phi}(3H - 6a^2H - 90) + k^2\Phi(18a^2H\\
&+ \frac{3}{2}H - 15) + \Phi(15 + 6H^2)\bigg) = 0. \qquad (3.34)
\end{aligned}
$$

By assuming the sub-horizon limit $k \gg aH$, the (00) component of the metric field equation will be

$$a^2\delta\rho + 4k^2\Phi + 4a^2\acute{f}(-a^2k^2 + \Phi) = 0. \qquad (3.35)$$

In the sub-horizon limit, the expansion of universe should be neglected. As a result, the only terms will survive in the field equation are $\delta, \theta, \delta p, k^2$. The $(0i)$ components are not independent and can be obtained from (00) component and conservation equation. After sub-horizon limit, the (ii) component of the field equation will be

$$\delta p = 4\acute{f}\Phi(-k^2a^2 + \Phi). \qquad (3.36)$$

We have found that the anisotropic stress parameter $\eta_a = \frac{\Phi}{\Psi}$ is equal to 1, which is same as obtained in Einstein's GR.

3.4 $f(Q) = Qe^{\frac{\lambda Q_0}{Q^2}}$

By working with exponential model, we will analyze the cosmological implications of $f(Q)$ gravity. Here λ is the only model free parameter and $Q_0 = 6H_0^2$. For $\lambda = 0$, GR is recovered but not ΛCDM case as it does not contain hidden cosmological constant in $f(Q)$ form [37]. We will use the value of non-metricity scalar from case 1 and Eqs. (3.6), (3.7) and (3.8), the Friedmann, Raychaudhuri and conservation equations under this model will be

$$\rho = e^{\frac{\lambda}{H^2}}\bigg(3H^2 + 12\lambda\frac{1}{H^2} - 12\bigg), \tag{3.37}$$

$$p = e^{\frac{\lambda}{H^2}}\bigg(-3H^2 - 6\lambda H^2 - 4\lambda^2\dot{H} + 4\lambda^2\frac{\dot{H}}{H^2} - 2\dot{H} + 2\lambda\frac{\dot{H}}{H^2}\bigg), \tag{3.38}$$

$$\begin{aligned}\dot{\rho} + 3H(\rho + p) &= e^{\frac{\lambda}{H^2}}\bigg(\frac{2}{3H^3}(\frac{1}{3} - 12\lambda) - 8(1+\lambda)\frac{\ddot{H}\dot{H}}{H^4} + 144\lambda\frac{\dot{H}^2}{H^3} - \frac{\lambda}{H^2}(1 - \frac{2}{H^2})\\ &+ 16\lambda\frac{\dot{H}}{H^2}(\frac{1}{H^6} + \frac{6}{H} - \frac{7}{4}) + 4\dot{H}(1+\lambda) + 2\ddot{H}(1+\lambda) + 2\lambda\frac{\ddot{H}}{H^2} + 72\dot{H}H^3\bigg).\end{aligned} \tag{3.39}$$

Now using (3.9) in above equations, the above set of equations are modified as

$$h^2 = \frac{1}{e^{\frac{\lambda}{h^2}}(\frac{1}{2} + \lambda)}\bigg(\bar{\rho_m} + \bar{\rho_r} + \lambda e^{\frac{\lambda}{h^2}}\bigg), \tag{3.40}$$

$$h^2 = -\frac{1}{e^{\frac{\lambda}{h^2}}(1 + 2\lambda)}\bigg(\bar{\rho_r} + 6\frac{\dot{h}}{h^2} + 2\dot{h}(2\lambda^2 - 3) + 2\lambda\bigg), \tag{3.41}$$

$$\acute{\bar{\rho_r}} + 4h\bar{\rho_r} = 0, \tag{3.42}$$

$$\begin{aligned}\acute{\bar{\rho_m}} + 3h\bar{\rho_m} &= e^{\frac{\lambda}{h^2}}\bigg(\frac{2}{3h^3}(\frac{1}{3} - 12\lambda) - 8\frac{\ddot{h}\dot{h}}{h^4}(1+\lambda) + 144\lambda\frac{\dot{h}^2}{h^3} - \frac{\lambda}{h^2}(1 - \frac{2}{h^2})\\ &+ 16\frac{\dot{h}\lambda}{h^2}(\frac{1}{h^6} + \frac{6}{h} - \frac{7}{4}) + 4\dot{h}(1+\lambda) + 2\ddot{h}(1+\lambda) + 2\frac{\lambda\ddot{h}}{h^2} + 72\dot{h}h^3\bigg),\end{aligned} \tag{3.43}$$

here prime represents derivative with respect to τ. For evolution of radiation density abundance, we will use Eq. (3.14).

Equations (3.40) and (3.41) in redshift coordinates can be written as, respectively

$$h^2 = \frac{2}{(1+2\lambda)e^{\frac{\lambda}{h^2}}}(\Omega_m + \Omega_{r0}(1+z)^4 + \lambda e^{\frac{\lambda}{h^2}}), \tag{3.44}$$

$$\begin{aligned}h^2(1+2\lambda)e^{\frac{\lambda}{h^2}} &- 2h\acute{h}(1+z)(2\lambda - 3)e^{\frac{\lambda}{h^2}} = -\Omega_{r0}(1+z)^4 + 2\lambda e^{\frac{\lambda}{h^2}}\\ &+ \frac{\acute{h}}{h}(1+z)(1+2\lambda)e^{\frac{\lambda}{h^2}}.\end{aligned} \tag{3.45}$$

Similarly, the conservation Eq. (3.43) for dust turn out to be

$$\begin{aligned}
(1+z)\Omega_m' + 3\Omega_m &= e^{\frac{\lambda}{h^2}}(1+z)^{-2}\Bigg(\frac{2}{3h^6} - 8\frac{\dot{h}}{h^{11}}(1+\lambda) + 144\lambda\frac{\dot{h}^2}{h^6} + 96\lambda\frac{\dot{h}}{h^6} + \frac{24\lambda}{h^6} \\
&+ 24\lambda(\frac{\dot{h}^2}{h^5}) + \frac{4}{h}(1+\lambda) + 2\frac{\ddot{h}}{h^3}(1+\lambda-\frac{\lambda}{h^2}) + 27\frac{\dot{h}}{h}(\frac{16}{3}+h+\frac{16\lambda}{3}) \\
&+ 4\frac{\lambda}{h^3}(36h-\frac{1}{h})\Bigg). \qquad (3.46)
\end{aligned}$$

The expression of h^2 can be obtained from Eq. (3.44) as given below

$$\begin{aligned}
h^2 &= \Bigg(\frac{1}{2}\Bigg(\frac{1}{\lambda+2}(-2\Omega_{m0}z^3 - 6\Omega_{m0}z^2 - 6\Omega_{m0}z - 2\Omega_{m0} - 2\Omega_{r0}z^3(1+z) - 2\Omega_{r0}z^2 \\
&\times (1+z) - 2\Omega_{r0}z(1+z) - 2\Omega_{r0}(1+z) + (1+z)^2+1)^2 + (\frac{2z^2}{\lambda+2})\Bigg) + \Bigg((4\Omega_{m0}z^3 \\
&+ 4\Omega_{m0}z^2 + 3\Omega_{m0}z + \Omega_{m0} + \Omega_{r0}z^3(1+z) + 3\Omega_{r0}z^2(1+z) + 2\Omega_{r0}z(1+z) + \Omega_{r0} \\
&\times (1+z))\frac{(\lambda+1)^2+1}{2}\Bigg)\Bigg). \qquad (3.47)
\end{aligned}$$

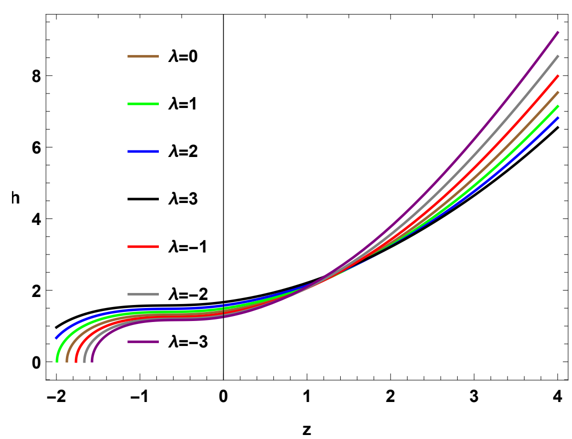

Figure 3.7: h versus z for different values of λ.

In Fig. **3.7**, we observe physical behavior of dimensionless Hubble parameter h. The Hubble function is positively increasing for all values of λ.

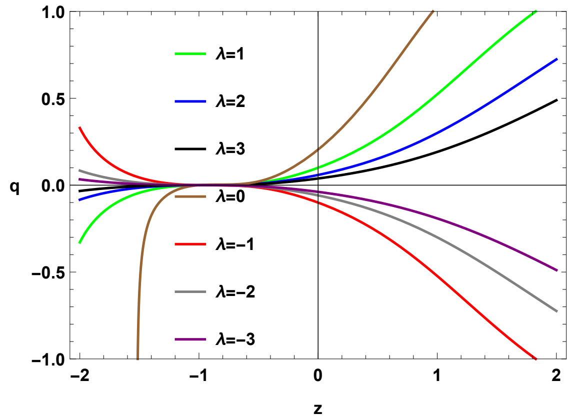

Figure 3.8: q versus z for different values of λ.

In Fig. **3.8**, graphical behavior of q is being presented. For positive values of λ, trajectories of q are shifting from decelerating phase to accelerating one from past to future, respectively. While an opposite behavior has been observed for negative values of λ. Hence, the exponential $f(Q)$ model produce physical results.

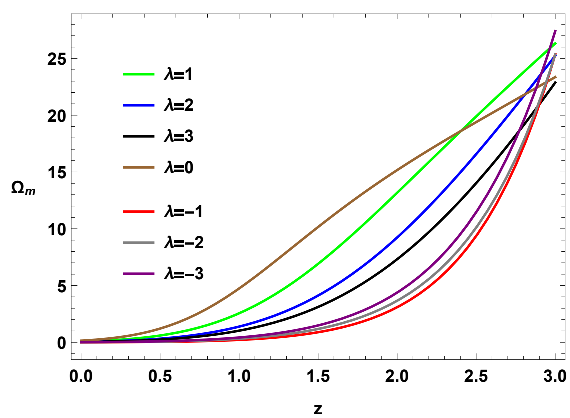

Figure 3.9: Dust abundance along z for different values of λ.

In Fig. **3.9**, we analyze the graphical behavior of dust abundance. We can observe that trajectories are showing increasing behavior for high redshift.

3.5 Dynamical System Analysis

By using the parameters given in (3.21) in (3.40), we generate following equation

$$1 = \Omega_m + \Omega_r + \Omega_h^{-1}\lambda e^{\frac{\lambda}{h^2}} - \frac{3}{2}a^2 e^{\frac{\lambda}{h^2}}. \tag{3.48}$$

The set of three independent dynamical equations Ω_m, Ω_r and Ω_h is as follows

$$\begin{aligned}
\Omega'_m &= \Omega_{m0}\bigg(-2-\frac{+3\Omega_{r0}+\Omega_{m0}+\lambda e^{\lambda}}{-2(2\lambda-3)e^{\lambda}-(1+2\lambda)e^{\lambda}}\bigg)+116\lambda \\
&+ \lambda\Omega_{h0}^{-1}\bigg(\frac{2}{3}+62(\frac{-3\Omega_{r0}-\Omega_{m0}-\lambda e^{\lambda}}{}-2(2\lambda-3)e^{\lambda}-(1+2\lambda)e^{\lambda})\bigg) \\
&+ \frac{326\lambda}{3}\bigg(\frac{-3\Omega_{r0}-\Omega_{m0}-\lambda e^{\lambda}}{-2(2\lambda-3)e^{\lambda}-(1+2\lambda)e^{\lambda}}\bigg), \qquad (3.49) \\
\Omega'_r &= \Omega_{r0}\bigg(-2-2(\frac{-3\Omega_{r0}-\Omega_{m0}-\lambda e^{\lambda}}{-2(2\lambda-3)e^{\lambda}-(1+2\lambda)e^{\lambda}})\bigg), \qquad (3.50) \\
\Omega'_h &= \Omega_{h0}\bigg(-2+2(\frac{-3\Omega_{r0}-\Omega_{m0}-\lambda e^{\lambda}}{-2(2\lambda-3)e^{\lambda}-(1+2\lambda)e^{\lambda}})\bigg), \qquad (3.51)
\end{aligned}$$

here prime represents the derivative with respect to $\ln a$. The EoS parameter for this model is

$$\omega_{eff} = 1 + \frac{2}{3}\bigg(\frac{3\Omega_{r0}+\Omega_{m0}+\lambda e^{\lambda}}{2(2\lambda-3)e^{\lambda}+(1+2\lambda)e^{\lambda}}\bigg). \tag{3.52}$$

3.5.1 Radiation Fixed Point (P_r):

The fixed point of dynamical system (3.49)-(3.51) is

$$P_r = (\Omega_m, \Omega_r, \Omega_h) = (0, 1, 0). \tag{3.53}$$

The point $(0,1,0)$ corresponds to a radiation dominated universe ($\omega_{eff} = \frac{1}{3}$). In this case, the eigenvalues are $(-1,-6,0)$, indicating that the radiation fixed point is saddle.

3.5.2 Dust Fixed Point (P_m):

$$P_m = (\Omega_m, \Omega_r, \Omega_h) = (1, 0, 0). \tag{3.54}$$

The point $(1, 0, 0)$ corresponds to a matter dominated cosmos. Here, eigenvalues are $(2, -8, 0)$, illustrating that dust fixed point is also saddle.

3.5.3 $Om(z)$ and Statefinder Parameter Diagnostic

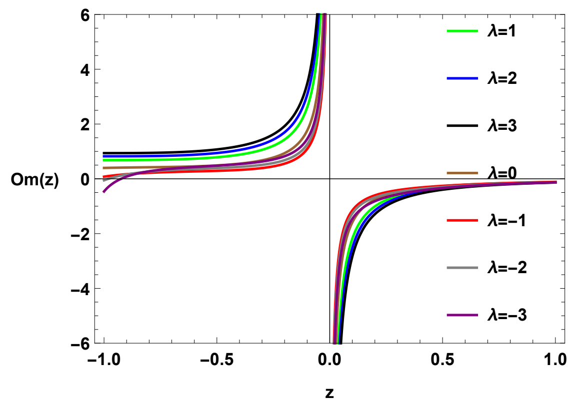

Figure 3.10: Om versus z corresponding to different values of λ.

In Fig. **3.10**, we can observe that trajectories are showing positive slope in future, which tends to phantom era for all chosen values of model parameter λ. The negative slope in past describes the quintessence era.

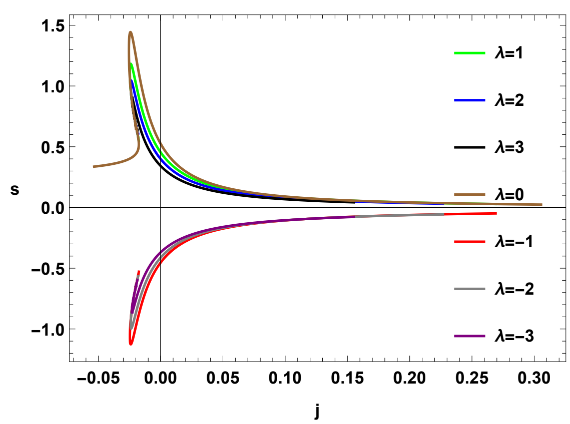

Figure 3.11: Parametric plot of j and s.

In Fig. **3.11**, initially $j, s > 1$, so graph does not fulfill any described physical region, but later it falls in $j < 1$ and $s > 0$ region, so trajectories represent quintessence and phantom-like behavior. For negative values of λ, trajectories fall in $j > 1$ and $s < 0$ region (exhibiting Chaplygin gas behavior).

3.5.4 Square Speed of Sound

We plot the graph of v_s^2 shown in Fig. **3.12**.

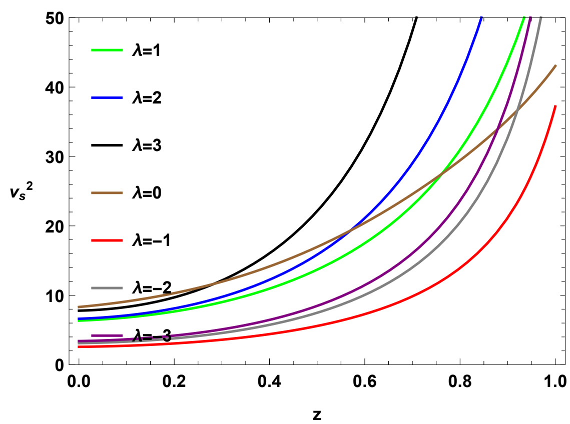

Figure 3.12: Graph of v_s^2 versus z.

For this model, we develop expression of v_s^2 by using ρ and p given in Eqs. (3.37) and (3.38), respectively. In Fig. **3.12**, $v_s^2 > 0$, which verifies the stability of model in past for all selected values of model parameter λ.

Chapter 4

Final Results

The major goal of this thesis is to determine the effectiveness of modified gravities in describing the accelerated expansion of cosmos. Although the scenarios of cosmic expansion has been extensively discussed in GR but there is a room to discuss it in modified theories of gravity. Modified theories of gravity have demonstrated their significance by introducing many interesting phenomena of the universe. One of modified theories is symmetric teleparallel gravity where one thinks about zero curvature and torsion. So we decided to analyze cosmology in $f(Q)$ gravity by taking flat FRW space-time. By considering perfect fluid distribution, the appropriate dynamical field equations and conservation equation have been obtained in this framework.

In **chapter 3**, we have discussed the expansion of cosmos by using two different $f(Q)$ models in FRW universe. We examined the role of these models by developing some cosmological parameters such as Hubble, deceleration, $Om(z)$ and the statefinder diagnostic parameters. The stability of the system is checked by evaluating the fixed points. From graphical analysis of these parameters, we have observed the behavior of cosmos.

The graphical description for $f(Q) = Q + \alpha Q^2$ model is described as:

- In Fig. **3.1**, we plotted the dimensionless Hubble parameter and observed that for all considered values of α the behavior is positive from past to future, representing expanding cosmos.

- In Fig. **3.2**, we observed a phase transition of deceleration parameter from decelerated to accelerated phase from past to future for all considered values of model parameter α.

- In Fig. **3.3**, we analyzed the graphical behavior of dust abundance, which is found to decrease as we approach future era.

- In Fig. **3.4**, trajectories of $Om(z)$ are exhibiting positive slope in future, which indicate the phantom era and transiting from quintessence to phantom region in past.

- In Fig. **3.5**, trajectories exhibit Chaplygin gas behavior in the past.
- Figure **3.6** is showing unstable behavior of the model.

The graphical description for $f(Q) = Qe^{\frac{\lambda Q_0}{Q^2}}$ model is as follows:

- Figure **3.7** shows that the Hubble function is increasing function of z.
- In Fig. **3.8**, we observed that the trajectories of q are transiting from decelerating to accelerating phase from past to future for all positive values of λ. For negative values of λ, opposite trend has been observed.
- Figure **3.9** shows that dust abundance has increasing behavior in past for all considered values of λ.
- In Fig. **3.10**, $Om(z)$ parameter indicates phantom era in future while in past depicts the quintessence region.
- In Fig. **3.11**, graph lies in phantom and quintessence region for positive values of λ. For negative values the result is not physical.
- Figure **3.12** shows the stability of model in past for all chosen values of model parameter λ.

It is important to note here that our results reduce to original $f(Q)$ theory for $\lambda = 0 = \alpha$.

Bibliography

[1] Sutta, P., Astrophys. Space Sci. **4**(2019)171.

[2] Riess, A.G. et al., Astrophys. J. **116**(1998)1009.

[3] Perlmutter, S. et al., Astrophys. J. **517**(1999)565.

[4] Bamba, K. et al., Astrophys. Space Sci. **342**(2012)155.

[5] Li, M. et al., Commun. Theor. Phys. **56**(2011)525.

[6] Ade, P.A.R. et al., Astrophys. **571**(2014)67.

[7] Sahni, V. et al., J. Exp. Theor. Phys. Lett. **77**(2003)201.

[8] Buchdahl, H.A., Mon. Not. Roy. Astron. Soc. **150**(1970)1.

[9] Starobinsky, A. A., Pisma Zh. Eksp. Teor. Fiz. **30**(1979)719.

[10] Nojiri, S. and Odintsov, S.D., Phys. Rev. D **68**(2003)123512.

[11] Ferraro, R. and Fiorini, F., Phys. Rev. D **75**(2007)084031.

[12] Linder, E.V., Phys. Rev. D **81**(2010)127301.

[13] Bamba, K. et al., J. Cosmol. Astropart. Phys. **01**(2011)021.

[14] Bahamonde, B. et al., Eur. Phys. J. C **77**(2017)2.

[15] Harko, T. et al., Phys. Rev. D **84**(2011)024020.

[16] Shabani, H. and Farhoudi, M., Phys. Rev. D **88**(2013)044048.

[17] Nojiri, S. et al., Prog. Theor. Phys. Suppl. **172**(2008)81.

[18] Elizalde, E. et al., Class. Quant. Grav. **27**(2010)095007.

[19] Bamba, K. et al., Eur. Phys. J. C **67**(2010)295.

[20] Jimenez, J. B. et al., Phys. Rev. D **98**(2018)044048.

[21] Beltran, J. et al., Phys. Rev. D **101**(2020)103507.

[22] Lazkoz, R. et al., Phys. Rev. D **100**(2019)104027.

[23] Yixin, Xu. et al., Eur. Phys. J. C **79**(2019)708.

[24] Lin, R. H., and Zhai, X. H., Phys. Rev. D **103**(2021)124001.

[25] Khyllep, W. et al., Phys. Rev. D **103**(2021)103521.

[26] Mandal, S. et al., Phys. Rev. D **102**(2020)024057.

[27] Lu, J. et al., Eur. Phys. J. C **79**(2019)530.

[28] Bajardi, F., Vernieri, D. and Capozziello, S., Eur. Phys. J. Plus **135**(2020)912.

[29] Jarv, L. et al., Phys. Rev. D **97**(2018)124025.

[30] Runkla, M. and Vilson, O., Phys. Rev. D **98**(2018)084034.

[31] Gakis, V. et al., Phys. Rev. D **101**(2020)064024.

[32] Harko, T. et al., Phys. Rev. D **98**(2018)084043.

[33] Ayuso, L. et al., Phys. Rev. D **103**(2021)063505.

[34] Hassan, Z. et al., Fortschritte der Phys. k. **69**(2021)2100023.

[35] Barros, B. et al., Phys. Dark Uni. **30**(2020)100616.

[36] Lu, J. et al., Eur. Phys. J. C **79**(2019) 530.

[37] Anagnostopoulos, F. et al., Phys. Lett. B **822**(2021)136634.

[38] Zhao, D. et al., Eur. Phys. J. C **82**(2022)4.

[39] Schwarz, P. M., Schwarz, J. H., *Special relativity from Einstein to strings* (Cambridge University Press, 2004).

[40] Puri, S.P., *General Theory of Relativity* (Dorling Kindersely India, 2013).

[41] Amendola, L., and Tsujikawa, S., *Dark energy: theory and observations* (Cambridge University, 2010).

[42] Mavromatos, N. E. et al., Int. J. Mod. Phys. D **26**(2017)1730007.

[43] https://evodevouniverse.com/blog/wp-content/uploads/2017/05/history-of-the-universe-PDG-LBNL2014-500.

[44] Frieman, J.A., Turner, M.S., Huterer, D., Ann. Rev. Astro. Astrophys. **46**(2008)385.

[45] Roos, M., *Introduction to cosmology* (John Wiley and Sons, 2015).

[46] https://gadgets360.com/science/news/universe-dark-matter-mass-ucr-galaxy-clusters-2303124.

[47] Chen, Y., Kumar, S. and Ratra, B., Astrophys. **835**(2017)86.

[48] Shahidi, S., Phys. Rev. D **104**(2021)084033.

[49] Sahoo, P., et al., arXiv:2110.11768.

[50] Kurki-Suonio, H., *Cosmological perturbation theory* (Lecture Notes for a Course of Cosmological Perturbation Theory given at the University of Helsinki, 2015).